Heliyon 10 (2024) e34030

Contents lists available at ScienceDirect

Heliyon

journal homepage: www.cell.com/heliyon

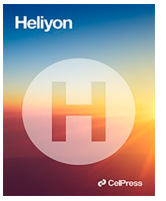

Research article

GL-V9 induce apoptosis of CML cells via MAPK signaling pathway

Fengyu Jiang [a,1], Yangyang Xue [a,1], Qin Zhang [a], Tonghui Ma [a], Yongming Li [a,**], Xiaoxuan Yu [a,b,*]

[a] Jiangsu Collaborative Innovation Center of Chinese Medicinal Resources Industrialization, School of Medicine, Nanjing University of Chinese Medicine, Nanjing, 210023, PR China
[b] State Key Laboratory of Pharmaceutical Biotechnology, School of Life Sciences, Nanjing University, Nanjing, 210023, PR China

ARTICLE INFO

Keywords:
GL-V9
CML
Apoptosis
MAPK

ABSTRACT

GL-V9, a derivative of wogonin, has shown potent antitumor effects in various cancers, yet its impact on chronic myeloid leukemia (CML) remains unexplored. In this study, we found that GL-V9 significantly decreased the viability of CML cells. Annexin V/PI staining demonstrated that GL-V9 induced apoptosis in a concentration-dependent manner. The JC-1 assay indicated a significant reduction in mitochondrial membrane potential (ΔΨm) in cells treated with GL-V9. Additionally, GL-V9 altered reactive oxygen species (ROS) levels in CML cells. Through transcriptomic sequencing and Western blot analysis, we further revealed that GL-V9 activated the MAPK pathway. These results suggest that GL-V9 is a promising therapeutic candidate for CML.

1. Background

Chronic Myeloid Leukemia (CML) is a type of myeloproliferative neoplasm characterized by excessive production of myeloid cells [1]. The underlying mechanism of CML is the formation of the t (9; 22) (q34; q11) [2]. This translocation occurs between the *ABL* proto-oncogene, locates on chromosome 9, and the *BCR* gene, locates on chromosome 22. The genetic rearrangement leads to the creation of the *BCR-ABL* fusion gene, which is functionally an oncogene [3,4]. The Philadelphia Chromosome (Ph), a reciprocal translocation of chromosome 9 and chromosome 22 [5], is very commonly found in patients with CML, accounting for approximately 90 % of CML cases [6,7]. Its presence is not only a key diagnostic marker for CML but also plays a crucial role in the treatment of the disease [8]. The primary clinical treatment for CML involves the use of tyrosine kinase inhibitors (TKIs) [8]. Imatinib (IM), the first-generation TKI, has seen extensive use since it was first introduced. However, the effectiveness of IM therapy is not consistent across all patients, with some eventually developing resistance to TKIs. Research has shown that 50%–90% of TKI resistance is due to mutations in the *ABL* kinase domain, which modify the drug binding site and reduce its inhibitory function [9,10]. Second- and third-generation TKIs, such as Nilotinib and Bosutinib, have demonstrated efficacy against certain IM-resistant mutations but come with a distinct adverse event profile, including liver toxicity and elevated serum lipase levels [11–13]. Given the significant side effects and limitations associated with TKIs, there is an urgent need for alternative drugs and treatment strategies [14,15].

The MAPK pathway, also called the RAS-RAF-MEK-ERK cascade, is a series of protein kinases activated by extracellular signals. It

* Corresponding author. Jiangsu Collaborative Innovation Center of Chinese Medicinal Resources Industrialization, School of Medicine, Nanjing University of Chinese Medicine, Nanjing, 210023, PR China.
** Corresponding author.
E-mail addresses: lym-569@njucm.edu.cn (Y. Li), xxyu@njucm.edu.cn (X. Yu).
[1] Fengyu Jiang and Yangyang Xue contributed equally to this work.

https://doi.org/10.1016/j.heliyon.2024.e34030
Received 12 May 2024; Received in revised form 25 June 2024; Accepted 2 July 2024
Available online 3 July 2024

transmits these signals to the nucleus, regulating gene expression and cellular responses such as proliferation, differentiation, and survival. Functions to transmit upstream signals to its downstream effectors to regulate physiological process such as cell proliferation, differentiation, survival and death [16]. The activation of the MAPK pathway initiates from a conformational change of RAS. Activated RAF phosphorylates and actives MEK, activating directly causes the phosphorylation of ERK. ERK phosphates are activated on numerous substrates, from kinase to transcription factors, and are found as a primary kinase that controls numerous cellular processes due to the extensive identification properties of substrates [17].

Abnormalities in the MAPK pathway is associated with several tumors [18]. Previous studies have demonstrated a synergistic role of NOTCH and MAPK signaling in bladder cancer [19]. And another studies aimed to characterize cancer stem cells (CSCs) in human bladder cancer and explore regulation through the MAPK/ERK signal pathway [20]. Studies examine the effect on triptolide the regulation of MAPK/ERK signaling pathway, which plays a central role in modulating tumor cell proliferation and metastasis in Esophageal Squamous Cell Cancer (ESCC) [21]. Research also show thathuman estrogen sulfotransferase (EST) enzyme modulates MAPK pathway in human breast cancer cell line MCF-7 [22]. Additionally, there has been extensive research on MAPK in CML. MAPK pathway is activated in BCR-ABL expressing cells and plays a key role in the generation of the growth inhibitory effects of IFN-a in CML cells [23]. Research has indicated that Brassinin (BSN) could initiate apoptosis, autophagy, and paraptosis by modulating the MAPK signaling pathway in CML cells [24]. According to a study, nobilitinin (NOB) promotes megakaryotic isolation through the expression of EGR1 dependent on the MAPK/ERK pathway in human CML cells, and NOB combines with IM could synergistically reduce the viability of CML cells [25]. The above results indicates that multiple drugs play a positive role in the treatment of CML through MAPK signaling pathway, highlighting its importance forCML.

Natural compounds play a significant role in CML through diverse mechanisms. For instance, gambogic acid induce CML cell and imatinib-resistant CML cell autophagy and apoptosis [26,27]. Atractylodes Rhizoma is one of the common medicines used to treat abdominal pain in traditional Chinese medicine. Atractylenolide (ATL-1), the active ingredient of Atractylodes Rhizoma, has been reported to be cytotoxic to CML cells, and can induce apoptosis and cell differentiation [28]. Glaucocalyxin A (GLA), a naturally

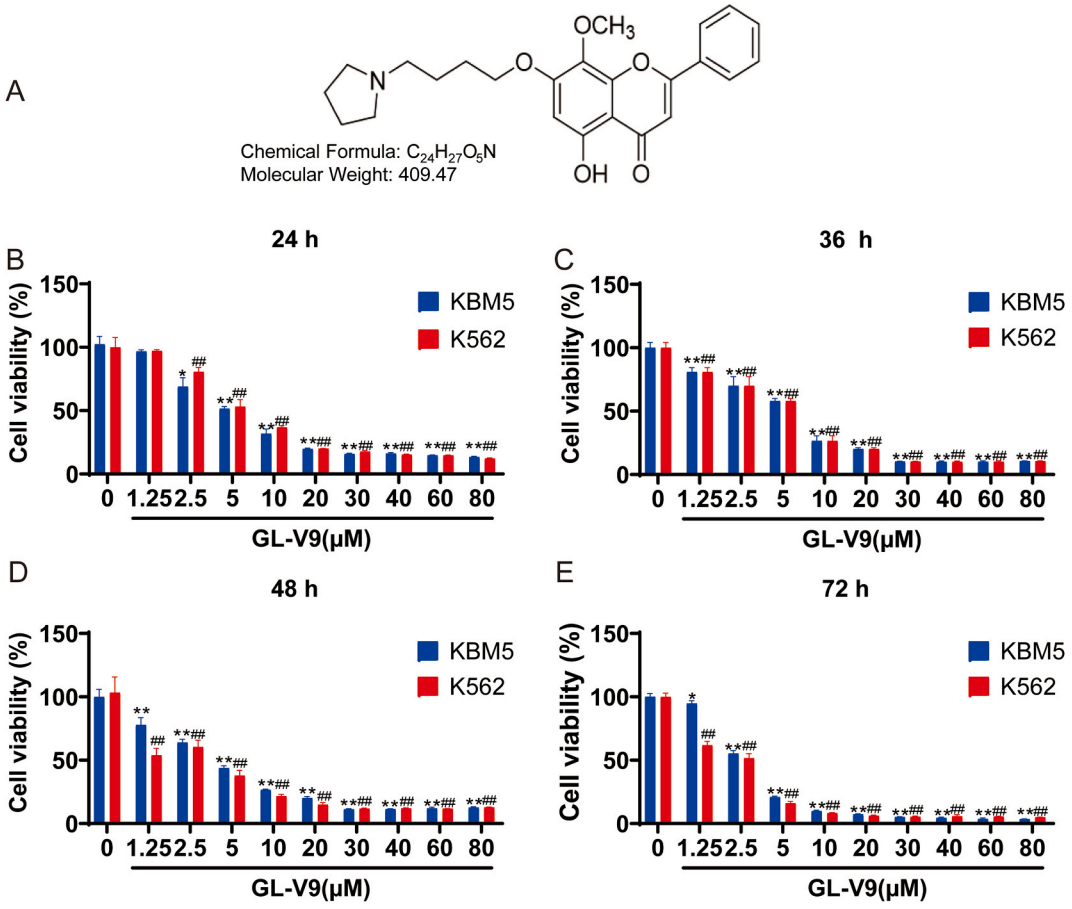

Fig. 1. The effects of GL-V9 of CML cells. (A) The chemical structure of GL-V9 ($C_{24}H_{27}O_5N$) is depicted. (B–E) The KBM5 and K562 cell lines were treated with GL-V9 for 24, 36, 48 and 72 h, and the cell viability was assessed using the CCK-8 assay. The data represent the mean ± SEM of three different experiments. Asterisks denote statistically significant *P < 0.05; **P < 0.01 in KBM5 cell line and $^{\#}$P < 0.05; $^{\#\#}$P < 0.01 in K562 cell line; Differences compared with controls by one-way ANOVA.

occurring bioactive compound extracted from the Rabdosia rubescens plant, exhibits potent anticancer property. GLA has shown to inhibit the proliferation of CML cells and induce mitochondria-dependent apoptosis [29]. Additionally, Dihydroartemisinin (HAD) has demonstrated inhibition of *BCR-ABL* gene fusion at the mRNA level in CML cells, leading to cell death [30]. These findings suggest that natural compounds play a significant role in the treatment of CML.

Flavonoids, including wogonin, wogoninside, oroxylin A, and baicalein, exhibit significant antitumor activity [31]. Research demonstrates that wogonin induces apoptosis in MDA-MB231 human breast cancer cells [32]. Additionally, the MAPK/ERK pathway plays a crucial role in wogonin-stimulated apoptosis of MDA-MB231 cell [33]. Furthermore, wogonin has been shown to reverse drug resistance in CML cells to IM by modulating the TGF-β/Smad4/Id3 pathway and reducing the expression of CXCR4 and CXCR7 [34]. As a representative flavonoid, wogonin and its derivatives have demonstrated anti-leukemia effects. For instance, LW-213, a wogonin derivative, induces G2/M phase cell cycle arrest in K562 and K562r cells by decreasing the function of the Cyclin B1/CDC2 complex [35]. These findings suggest that flavonoids have significant potential in the treatment of CML.

GL-V9 is a novel synthesized flavonoid (Fig. 1A), has attracted attention for its antitumor effects in various cancer cells [36]. It demonstrates antiproliferative properties, induces cell cycle arrest, inhibits invasion, and promotes autophagy [37]. Studies shown that GL-V9 suppresses the activation of the AR-AKT-GK2 signaling axis and triggers glycolytic inhibition as well as mitochondrial-driven apoptosis [38]. GL-V9 also mitigates liver fibrosis by blocking the activation of hepatic stellate cells (HSCs) through binding to TGFβRI and subsequently inhibiting TGF-β/Smad pathway [39]. While GL-V9 plays an anti-tumor role in a variety oncology settings, the mechanisms underlying its effect on CML cells not been fully elucidated.

In this study, we investigated the fundamental anti-CML effects of GL-V9 and preliminarily explored its mechanism of action using transcriptomic sequencing. Our findings provide new insights for the clinical treatment of CML.

2. Methods

2.1. Reagents and antibodies

GL-V9 with >98 % purity by HPLC were kindly provided by Dr. Zhiyu Li (China Pharmaceutical University, Nanjing, China) and dissolved in DMSO (Sigma-Aldrich, St. Louis, MO, USA) as stock solution at 50 mM. Antibodies against Primary antibodies for Bax (Santa, SC-7480), Bcl-2 (Santa, SC-7382), PARP-1 (Proteintech, 66520-1-LG). JNK (Cell Signaling, 9252), phosphorylation-JNK (Thr183/Tyr185) (Cell Signaling, 4668), p38 (Cell Signaling, 9212), phosphorylation-p38 (Thr180/Tyr182) (Cell Signaling, 8690), ERK(Cell Signaling, 4695), phosphorylation-ERK (Thr202/Tyr204) (Cell Signaling, 4370).

2.2. Cell and culture

The human CML cell lines KBM5 and K562 were obtained from the Cell Bank of the Shanghai Institute of Biochemistry & Cell Biology. These cells were cultivated in a suspension culture format using RPMI-1640 medium (GIBCO, USA), which were supplemented with 10 % fetal bovine serum (FBS) (Life-iLab, China) and 100 U/mL of Penicillin-Streptomycin solution. The cell cultures were kept in an environment of 5 % carbon dioxide and 95 % air with a humidified atmosphere at a temperature of 37 °C. All the cells used in our experiments were passaged in our laboratory for a duration of three months or less after they were revived from cryopreservation.

2.3. Western blot analysis

Harvest cells and perform triple wash with PBS. Prepare protein lysis buffer (Yeasen, 20101ES60), including protease (Yeasen, 20124ES03) and phosphatase inhibitors (Yeasen, 20109ES05). Resuspend cells in an appropriate volume of protein lysis buffer, incubate on ice for 50 min with shaking every 25 min. Centrifuge cells at 13,000 rpm, 4 °C for 30 min. Utilize a BCA assay kit (Yeasen, 20201ES76) to determine protein concentration in the supernatant and measure OD values with a spectrophotometer.

2.4. Cell proliferation assays

The effects of GL-V9 on the proliferation of KBM5 and K562 cells were evaluated using the CCK-8 (Targetmol, C0005) assay. Cells were plated into each well of a 96-well plate and then compound at the specified concentration was added to each well. The cells were then incubated in a CO_2 incubator for the predetermined duration. After the designated incubation time, 20 μL of CCK-8 reagent was added to each well, and the plates were further incubated for an additional 4 h. The absorbance at 450 nm was finally measured using a Spectrum instrument (Allsheng, China). The inhibition rate of GL-V9 on the growth of KBM5 and K562 cells was calculated as a percentage of the control values.

2.5. Flow cytometric analysis of apoptosis

To assess cell apoptosis, cells were harvested and combined with the Annexin V/Propidium Iodide (PI) Cell Apoptosis Detection Kit (Vazyme Biotec, A211-01) as directed by the manufacturer. This process involved a 10-min incubation at room temperature in the dark. Data capture and analysis were carried out using a BD Accuri C6 Plus flow cytometer equipped with CellQuest software. Cells were considered viable if they did not stain with both Annexin V and PI.

2.6. Detection of the intracellular ROS level

Cellular reactive oxygen species (ROS) levels were quantified using the fluorescent dye 2′,7′-dichlorofluorescein diacetate (DCFH-DA) (Beyotime, S0033 M), following the supplier's protocol. Post-treatment, cells were mixed with DCFH-DA, Data capture and analysis were carried out using a BD Accuri C6 Plus flow cytometer equipped with CellQuest software.

2.7. Measurement of the mitochondrial membrane potential

Following treatment with BTZ, the cells were collected and incubated with 10 μM JC-1 dye (Beyotime, C2005) using the manufacturer's recommended protocol. After the staining process, the cells were then analyzed using flow cytometry, with excitation at 488 nm and emission detection at 530 nm, utilizing the FL-1 (green) and FL-2 (red) channels.

2.8. Transcriptome sequencing and bioinformatics analysis

Transcriptome sequencing and bioinformatics analysis were completed by Jiangbei New Area Biopharmaceutical Public Service Platform (2022-PJXM111-NJUCM). The cDNA samples from all subjects were sequenced on the Illumina NovaSeq 6000 platform. These raw reads underwent rigorous quality control and alignment processes to the reference genome to filter out noise and obtain high-quality data for further analysis. Subsequent this, the mapped reads were functionally annotated using both the Gene Ontology (GO) and Kyoto Encyclopedia of Genes and Genomes (KEGG) databases. To identify differentially expressed genes (DEGs) between groups, the DESeq2 package was employed. Thereafter, comprehensive functional enrichment analyses, including GO and KEGG databases exploration, were conducted in sequence to elucidate the underlying biological processes and pathways.

3. Results

3.1. GL-V9 inhibited cell viability of in CML cells

The growth-inhibitory effect of GL-V9 on CML cell lines was evaluated by conducting CCK-8 assay. K562 and KBM5 cells were exposed to various concentrations of GL-V9 (0–80 μM) for 24, 36, 48 and 72 h. As shown in Fig. 1, the cell viability of these cell lines was significantly diminished by GL-V9 in a time- and concentration-dependent manner. Furthermore, the half maximal inhibitory concentration (IC_{50}) values of GL-V9 on K562 cells were 7.10 ± 0.78 μM, 3.82 ± 0.59 μM, 2.94 ± 0.37 μM, 1.84 ± 0.29 μM after 24,

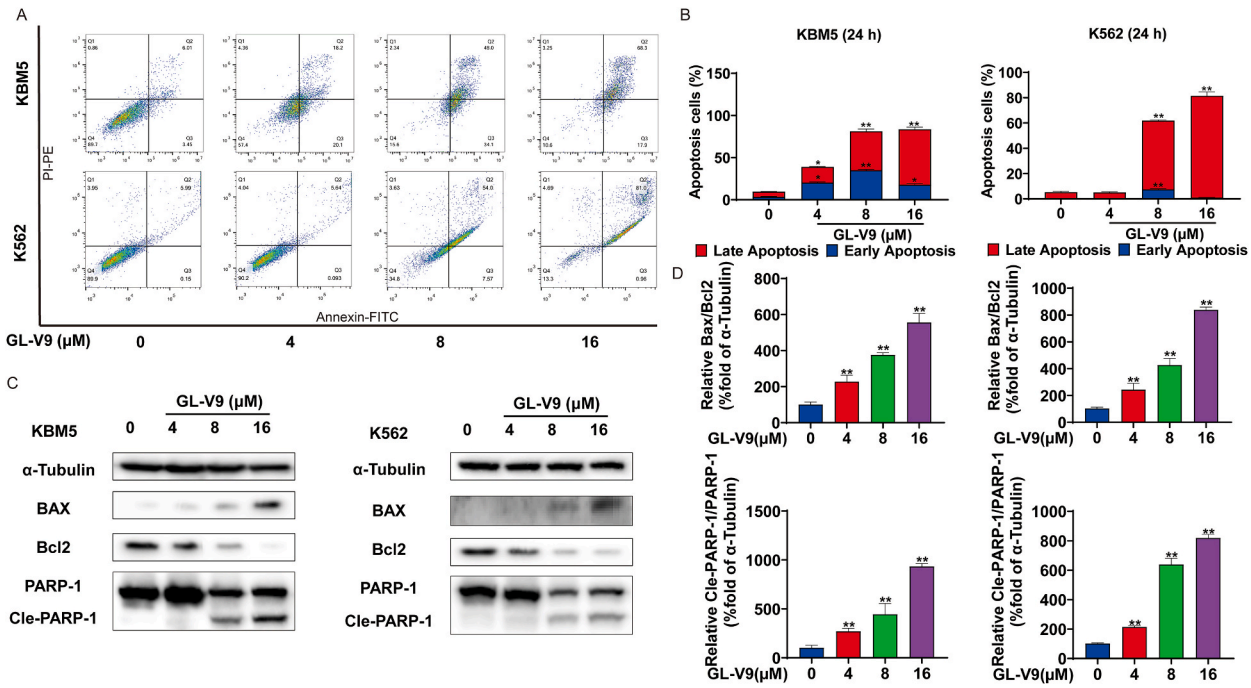

Fig. 2. GL-V9 induced apoptosis of CML cells. (A, B) Flow cytometric analysis of Annexin V-FITC/PI-PerCP- stained CML cell lines (KBM5 and K562) treated with GL-V9 (0, 4, 8, 16 μM) for 24 h. (C, D) KBM5 and K562 cell lines were treated with GL-V9 (0, 4, 8 and 16 μM) for 24 h, Western blot analysis of Bax, Bcl-2 and Cleaved-PARP-1 expression and activity quantification. α-Tubulin were used as loading controls. The data represent the mean ± SEM of three different experiments. Asterisks denote statistically significant *P < 0.05; **P < 0.01; Differences compared with controls by one-way ANOVA.

36, 48, and 72 h of treatment, respectively. In KBM5 cells, the IC_{50} values under the same conditions were 6.10 ± 0.71 μM, 5.29 ± 0.62 μM, 4.23 ± 0.43 μM, 2.87 ± 0.32 μM (Fig. 1B–E). Consequently, it was observed that GL-V9 exhibited notable inhibitory effects on CML.

3.2. GL-V9 induced cell apoptosis in CML cells

Apoptosis, a form of programmed cell death, is a pivotal mechanism within various anti-tumor research. We then determined the optimal condition for GL-V9 to induce apoptosis in CML cell lines K562 and KBM5. To further evaluate the apoptosis-inducing effect on GL-V9 on CML cells, we assessed the degree of apoptosis using flow cytometry. The Annexin V/PI double-staining assay, a widely utilized method for detecting apoptosis, demonstrated a concentration-dependent induction of apoptosis by GL-V9 in CML cells (Fig. 2A and B).

The ratios of early apoptosis in KBM5 cells were 3.4 ± 0.26 %, 20.33 ± 0.87 %, 3503 ± 1.00 %, 17.83 ± 1.40 %. And the late apoptpsis ratios were 6.07 ± 0.14 %, 18.63 ± 0.59 %, 46.27 ± 2.66 %, 65.8 ± 2.73 % after GL-V9 treatment (0, 4, 8 and 16 μM) for 24 h. As for K562 cells, the ratios of early apoptosis were 0.22 ± 0.07 %, 0.18± 0.01 %, 7.46 ± 0.5 %, 1.00 ± 0.08 % andthe late apoptosis ratios were 5.44 ± 0.49 %, 5.29 ± 0.51 %, 54.47 ± 0.57 %, 80.43 ± 2.99 %. Western blotting analysis was performed to examine the changes in the expression of apoptosis-related proteins in K562 and KBM5 cells following treatment with 0, 4, 8, and 16 μM GL-V9 for 24 h. The results showed an upregulation of Bax protein expression and a downregulation of Bcl-2 expression, resulting in an increased Bax/Bcl-2 ratio, indicating that GL-V9 induced apoptosis in CML cells KBM5 and K562. Furthermore, there was a downregulation of PARP-1 and a significant upregulation of cleaved-PARP-1, leading to an increased cleaved-PARP-1/PARP-1 ratio. (Fig. 2C and D,

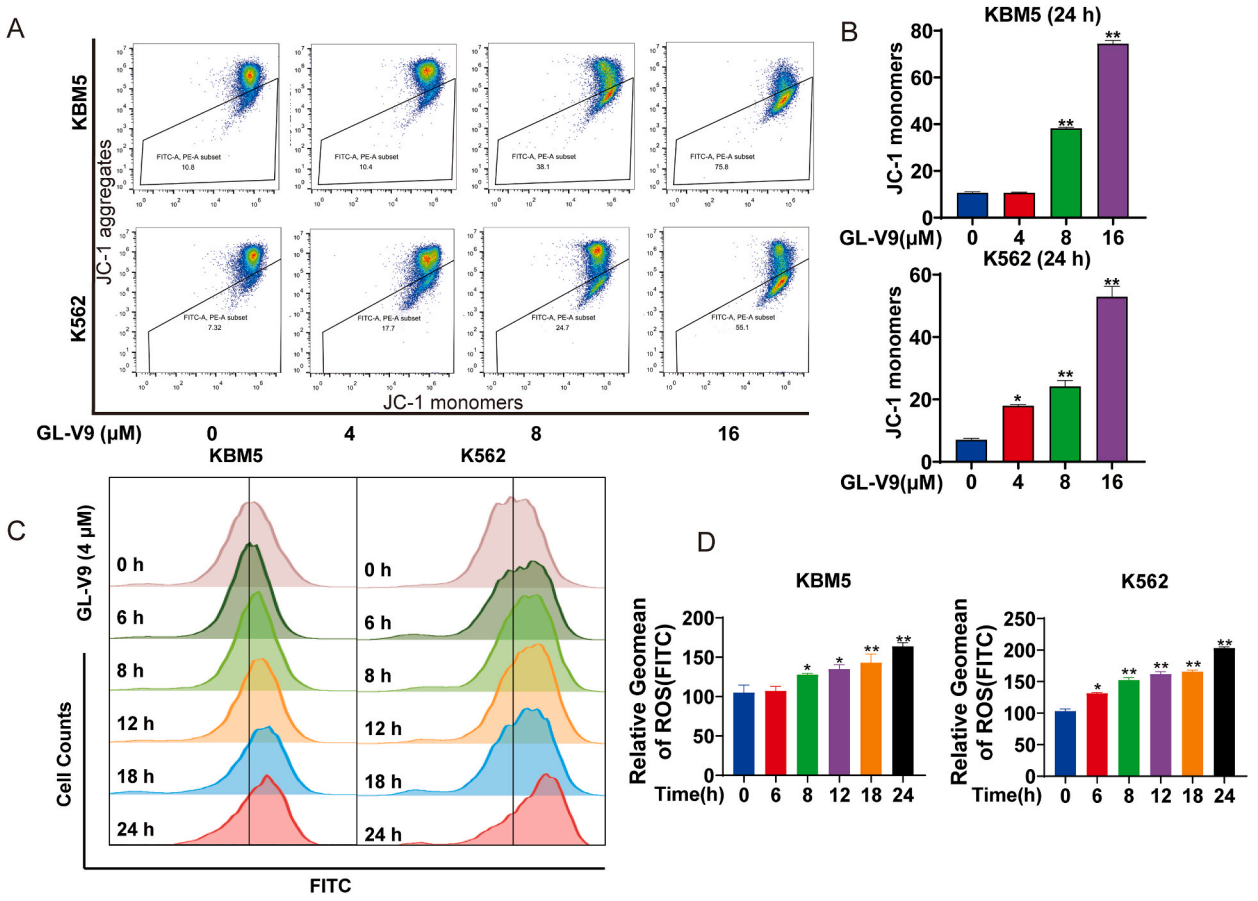

Fig. 3. GL-V9 leaded to the collapse of mitochondrial membrane potential and increased cellular reactive oxygen species levels in CML cell. (A, B) KBM5 and K562 cells were treated with GL-V9 (0, 4, 8 and 16 μM) for 24 h, and the changes in the ΔΨm of KBM5 and K562 cells were detected by JC-1 staining and analyzed by flow cytometry. The relative ΔΨm was calculated as the ratio of red fluorescence in treated cells to that in DMSO control cells. (C, D) Fluorescence microscope and flow cytometric analysis of the fluorescence intensity flow cytometry was utilized to measure the expression of ROS in KBM5 and K562 cells treated with GL-V9 (4 μM) for 24 h. The fold changes in ROS intensity values (% of control) were calculated.

The data represent the mean ± SEM of three different experiments. Asterisks denote statistically significant *P < 0.05; **P < 0.01; Differences compared with controls by one-way ANOVA.

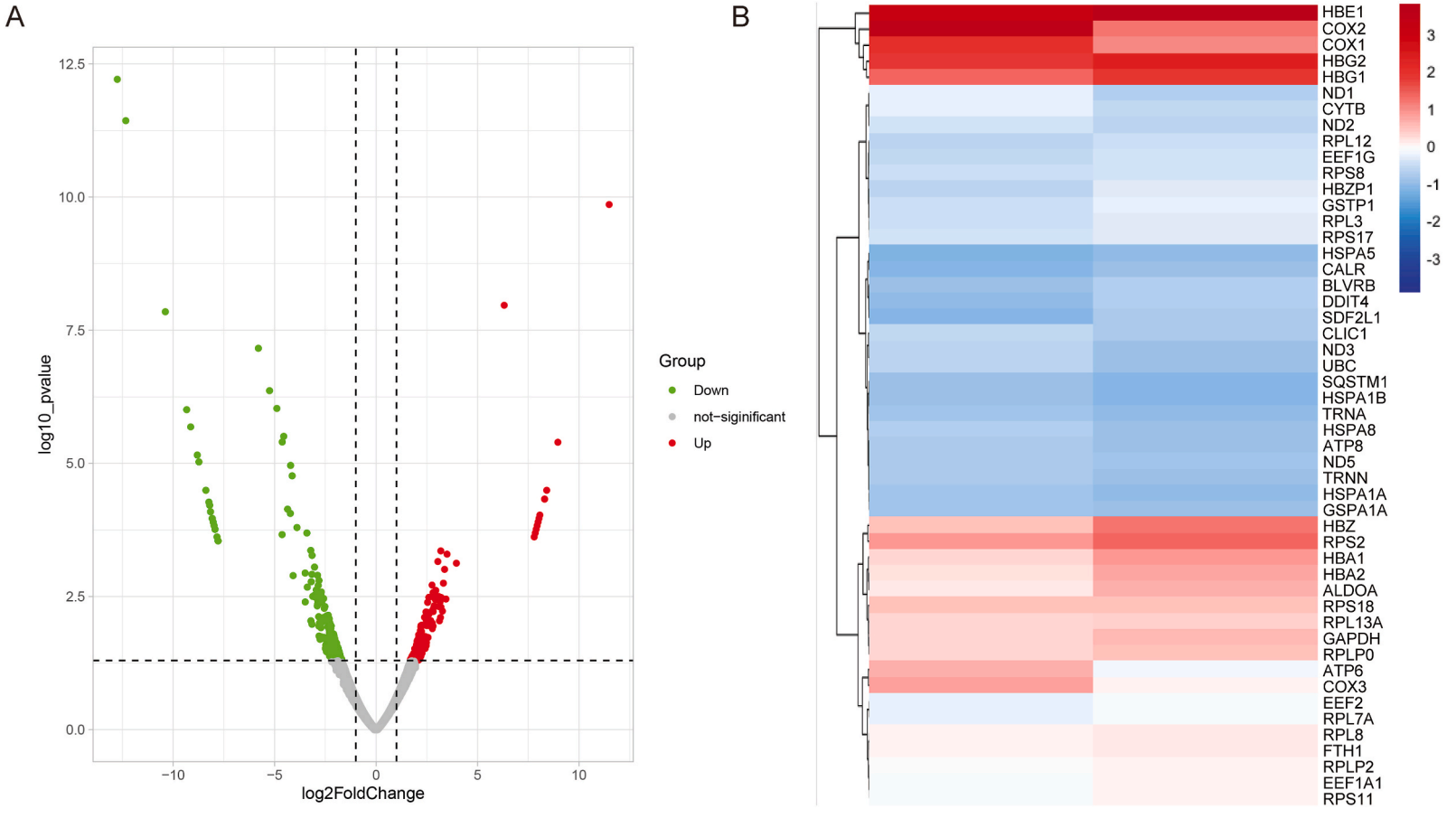

Fig. 4. GL-V9 induced genes changes in CML cell. KBM5 cells were exposed to 8 μM GL-V9 for 12 h, following which the sample were collected for transcriptome sequencing and subsequent bioinformatics analysis. (A) The red points in the graph indicates up-regulated gene, the green points down-regulated gene and the gray points non-significant, as shown in the Volcano map. (B) The heat map displays the top 50 genes that changed in KBM5 cells treated with GL-V9.

Supplementary Figs. 1–2). These results indicated that GL-V9 effectively induced apoptosis in CML cell lines.

3.3. GL-V9 caused collapse of mitochondrial membrane potential in CML cells

In the process of cell apoptosis, mitochondrial damage often occurs and the mitochondrial membrane potential changes [40]. Subsequently, we investigated the cellular apoptotic mechanisms, with a focus on early indicators such as mitochondrial damage. Consequently, we initially assessed the impact of GL-V9 on the mitochondrial membrane potential (ΔΨm) in CML cells. JC-1 results revealed that exposure to GL-V9 for 24 h resulted in a collapse of ΔΨm, indicating a significant incremental decrease in ΔΨm in GL-V9-treated cells. The membrane potential of KBM5 cells changed by 10.63 ± 0.38, 10.63 ± 0.21, 38.13 ± 0.45 and 74.41 ± 135 when GL-V9 was 0, 4, 8 and 16 μM, respectively, while that of K562 cells changed by 7.04 ± 0.46, 17.91 ± 0.42, 24.17 ± 1.81 and 52.93 ± 3.63 (Fig. 3A and B).

3.4. GL-V9 increased the intracellular levels of ROS in CML cells

Reactive oxygen species (ROS) refer to chemically active oxygen-containing substances, closely linked to the occurrence, development, and apoptosis of tumors [41].

To determine whether GL-V9 induced ROS formation in CTCL cells, we exposed K562 and KBM5 cells to 4 μM GL-V9 for 6, 8, 12, 18, and 24 h, and then measured the fluorescence intensity to assess ROS levels. The results showed that in KBM5 cells, the fluorescence intensity increased significantly at 8 h and continued to rise in a time-dependent manner, peaking at 24 h with approximately a 1.5-fold increase in ROS levels. In K562 cells, ROS levels began to increase at 6 h, peaking at 24 h with a doubling of ROS levels compared to untreated cells. These findings indicate that 4 μM GL-V9 induced a time-dependent increase in ROS levels in CML cells (Fig. 3C, D).

3.5. GL-V9 activated the MAPK pathway in CML cells

Transcriptome sequencing analysis was utilized to further investigate the anti-CML mechanism of GL-V9. Following treatment of

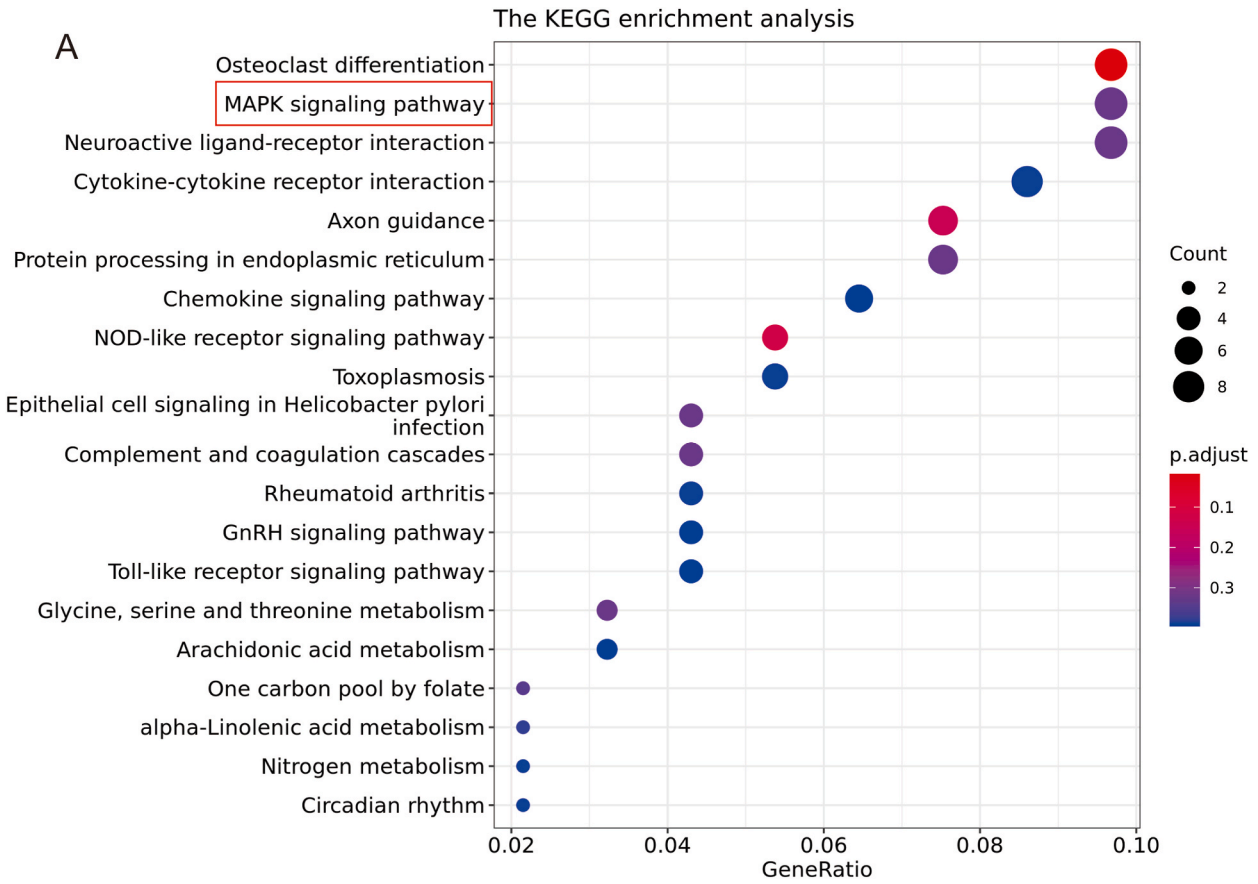

Fig. 5. GL-V9 affected the expression KEGG enrichment results in CML cells. (A) The x-axis represents the enriched KEGG pathways, with dot color indicating corrected significance (p-value) and dot size indicating the number of genes enriched in each pathway.

KBM5 cells were treated with 8 μM GL-V9 for 24 h, sequencing analysis revealed significant alterations in 377 genes, including 150 genes upregulated and 187 genes downregulated (Fig. 4A). We utilized DESeq2 to examine variance in gene expression levels. To identify genes that exhibited significant changes, we applied the following criteria: $|\log2FoldChange| > 1$, indicating a substantial alteration, and a *P*-value threshold of less than 0.05, indicating statistical significance. The results of heat map showed the changes of top 50 genes in KBM5 cells after GL-V9 treatment (Fig. 4B). We further investigated the impact of GL-V9 treatment on gene expression in CML cells and its effect on cell function. Subsequently, we performed KEGG pathway analysis on the differentially expressed genes and found that the MAPK signaling pathway was closely related to GL-V9-induced apoptosis in CML cells (Fig. 5). We then monitored key proteins related to the MAPK pathway and found that after treatment with 4, 8, and 16 μM GL-V9 for 24 h, the phosphorylation levels of JNK, p38, and ERK significantly increased in both KBM5 and K562 cells. Meanwhile, the levels of the unphosphorylated forms of JNK, p38, and ERK remained almost unchanged (Fig. 6A–D, Supplementary Figs. 3–4). These results indicated that GL-V9 can activate the MAPK pathway, suggesting that the MAPK pathway played a crucial role in GL-V9-induced apoptosis in CML cells.

4. Discussion

At present, tyrosine kinase inhibitors (TKIs) are commonly utilized in the clinical treatment of chronic myeloid leukemia (CML), with first-generation TKIs such as Imatinib (IM) and the second and third generation TKIs, such as Nilotinib and Bosutinib, have gradually emerged in clinical practice [42], which have demonstrated effective in cases of imatinib resistance. Nevertheless, these medications are associated with significant adverse reactions [43], which may prevent some patients from receiving treatment. Therefore, alternative treatments to TKIs are still needed for CML.

Flavonoids have shown great potential in treating CML. GL-V9, a wogonin derivative, has been investigated for its efficacy in various types of cancer. GL-V9 has been shown to induce apoptosis of prostate cancer cells [44], inhibit the migration and invasion of liver tumor cells [45]. The aim of this study is to reveal the signaling pathway and mechanism of GL-V9 against CML. In our study, our findings indicated that after GL-V9 treatment of CML cells, apoptosis was detected by flow cytometry, and both K562 and KMB5 cells showed varying degrees of apoptosis in a concentration-dependent manner. Consequently, it can be inferred that GL-V9 is capable of inducing apoptosis in CML cells.

Cells recognize to external signals by activating specific intracellular programs, including signaling cascades that trigger the activation of MAPK. Imatinib intolerance or primary resistance occurs, and many patients develop secondary resistance due to activation of intrinsic signaling pathways, including the JAK/STAT5, GSK3β and RAS/RAF/MAPK/ERK pathways. Studies have shown that down-regulating the expression of MAPK signaling pathway can inhibit the occurrence of BCR-ABL [46]. Studies have indicated that AMPK/MAPK/miR-22/HuR pathway induces apoptosis of CML cells [47], suggesting that the MAPK signaling pathway may be a

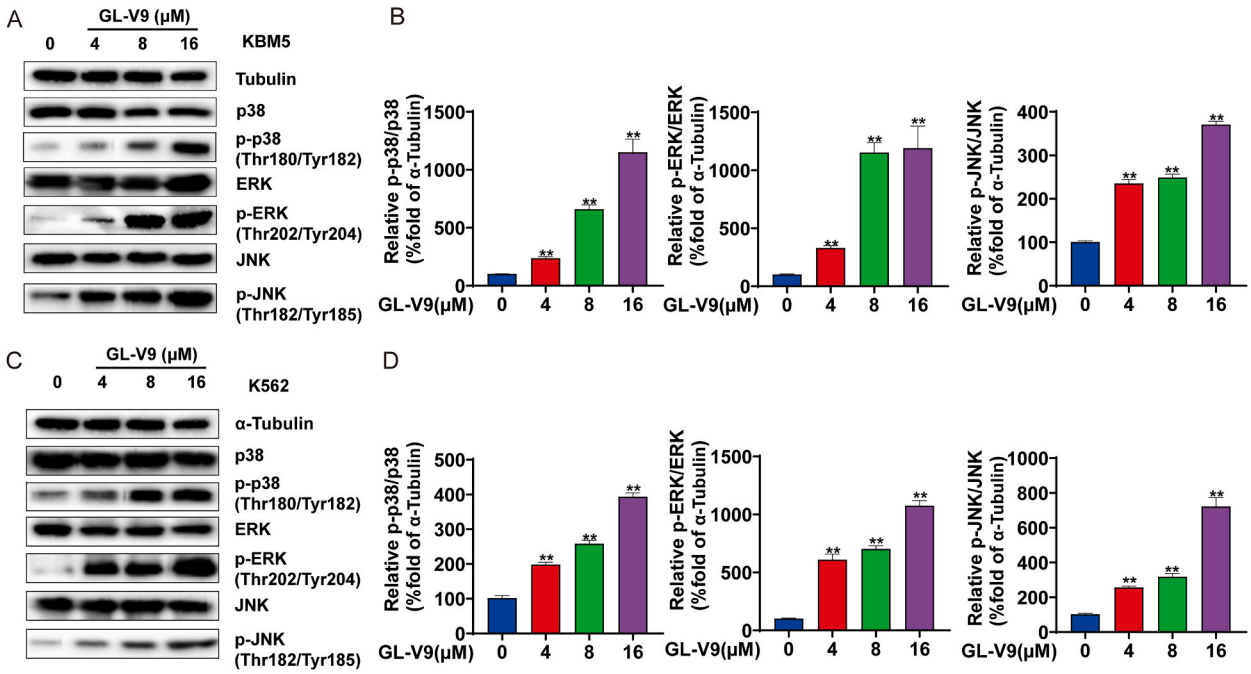

Fig. 6. GL-V9 induced MAPK pathway proteins expression in CML cells. (A, B) KBM5 cell lines were treated with GL-V9 (0, 4, 8 and 16 μM) for 24 h, Western blot analysis of p-38, *p*-p38, ERK, *p*-ERK, JNK and *p*-JNK expression. (C, D) K562 cell lines were treated with GL-V9 (0, 4, 8 and 16 μM) for 24 h, Western blot analysis of p-38, *p*-p38, ERK, *p*-ERK, JNK and *p*-JNK expression. α-Tubulin were used as loading controls.
The data represent the mean ± SEM of three different experiments. Asterisks denote statistically significant *P < 0.05; **P < 0.01; Differences compared with controls by one-way ANOVA.

feasible strategy for CML therapy.

In our study, we investigated the inhibitory effects of GL-V9 on the proliferation of CML cells, specifically KBM5 and K562, and found that it induces apoptosis in these cells, accompanied by ROS production. Additionally, transcriptome sequencing revealed that GL-V9 activates the MAPK pathway in CML cells, underscoring the crucial role of the MAPK signaling pathway in anti-CML therapy. Our research elucidates the anti-CML effects of GL-V9, providing new insights for CML treatment.

Data availability statement

The datasets used for the current study are available from the corresponding author on reasonable request. All data generated or analyzed during this study are included in this published article.

CRediT authorship contribution statement

Fengyu Jiang: Writing – review & editing, Writing – original draft, Visualization, Supervision, Software. **Yangyang Xue:** Data curation. **Qin Zhang:** Data curation. **Tonghui Ma:** Investigation, Conceptualization. **Yongming Li:** Investigation, Conceptualization. **Xiaoxuan Yu:** Funding acquisition, Data curation, Conceptualization.

Declaration of competing interest

The authors declare that they have no known competing financial interests or personal relationships that could have appeared to influence the work reported in this paper.

Acknowledgements

This work was supported by the National Natural Science Foundation of China (82204443), Natural Science Foundation of Jiangsu province (BK20210693), General Project of Basic Science in Colleges and Universities of Jiangsu Province (21KJB310013), Jiangsu Provincial Health Commission (Z2021064), the Priority Academic Program Development of Jiangsu Higher Education Institutions (Integration of Chinese and Western Medicine).

Appendix A. Supplementary data

Supplementary data to this article can be found online at https://doi.org/10.1016/j.heliyon.2024.e34030.

Abbreviations

CML	Chronic Myeloid Leukemia
ROS	Reactive Oxygen Species
MAPKs	Mitogen-Activated Protein Kinases
Ph	Philadelphia Chromosome
TKIs	Tyrosine Kinase Inhibitors
IM	Imatinib
CSCs	Cancer Stem Cells
ESCC	Esophageal Squamous Cell Cancer
BSN	Brassinin
NOB	Nobilitinin
HSCs	Hepatic Stellate Cells
DCFH-DA	2′,7′-Dichlorofluorescein Diacetate
GO	Gene Ontology
KEGG	Kyoto Encyclopedia of Genes and Genomes
ATL-1	Atractylenolide
GLA	Glaucocalyxin A
HAD	Dihydroartemisinin

References

[1] L. Steven, H. Gillian A, C. Mhairi, Targeting BCR-ABL1-positive leukaemias: a review article, Camb Prism Precis Med 1 (2024).
[2] C. Jorge, et al., Dynamics of BCR-ABL kinase domain mutations in chronic myeloid leukemia after sequential treatment with multiple tyrosine kinase inhibitors, Blood 110 (12) (2007) 4005–4011.
[3] A. Baassiri, et al., BCR::ABLThe molecular signature of and in a chronic myeloid leukemia model, iScience 27 (4) (2024) 109538.

[4] N. Huang, et al., Induction of apoptosis in imatinib sensitive and resistant chronic myeloid leukemia cells by efficient disruption of bcr-abl oncogene with zinc finger nucleases, J. Exp. Clin. Cancer Res. 37 (1) (2018) 62.
[5] A. Patel, et al., Pharmacotherapeutic options for Philadelphia chromosome- positive CML, J. Cancer Res. Updates 7 (2) (2018) 49–58.
[6] F. Mennini, et al., Budget Impact analysis of the first-line treatment of Philadelphia chromosome-positive chronic myeloid leukemia (Ph+ CML) adult patients, Farmeconomia Health economics and therapeutic pathways 18 (1) (2017).
[7] A. Hochhaus, et al., Molecular response with nilotinib in patients with Philadelphia negative (Ph-) chronic myeloid leukemia in chronic phase (CML-CP): ENEST1st sub-analysis, Blood 126 (23) (2015), 4054-4054.
[8] L. Bavaro, et al., Mechanisms of disease progression and resistance to tyrosine kinase inhibitor therapy in chronic myeloid leukemia: an update, Int. J. Mol. Sci. 20 (24) (2019).
[9] C. Tang, et al., Modelling of TKI resistance in CML cell lines: kinase domain mutations usually arise in the setting of BCR-ABL overexpression, Blood 116 (21) (2010), 3383-3383.
[10] M. Martinez-Castillo, et al., Genetic alterations in the BCR-ABL1 fusion gene related to imatinib resistance in chronic myeloid leukemia, Leuk. Res.: A Forum for Studies on Leukemia and Normal Hemopoiesis (2023) 131.
[11] J. Cortes, et al., Efficacy and safety of bosutinib (SKI-606) among patients with chronic phase Ph+ chronic myelogenous leukemia (CML), Blood 110 (11) (2007), 733-733.
[12] F. Castagnetti, et al., Dose optimization in elderly CML patients treated with bosutinib after intolerance or failure of first-line tyrosine kinase inhibitors, Blood 134 (Supplement_1) (2019), 496-496.
[13] A. Hochhaus, E. Eigendorff, T. Ernst, Chronische myeloische leukmie, TumorDiagnostik Ther. 40 (1) (2019) 43–49.
[14] A. Iurlo, et al., Impact of genetic predisposition on glyco-metabolic side effects of TKIs in CML, Blood 136 (Supplement 1) (2020), 5-5.
[15] M. Suttorp, M. Metzler, F. Millot, Horn of plenty: value of the international registry for pediatric chronic myeloid leukemia, World J. Clin. Oncol. 11 (6) (2020) 308–319.
[16] F. Liu, et al., Targeting ERK, an Achilles' Heel of the MAPK pathway, in cancer therapy, Acta Pharm. Sin. B 8 (4) (2018) 552–562.
[17] A.S. Dhillon, et al., MAP kinase signalling pathways in cancer, Oncogene 26 (22) (2007) 3279–3290.
[18] Q. Zheng, et al., Structure-based virtual screening for novel p38 MAPK inhibitors and a biological evaluation, Acta Materia Medica 2 (4) (2023) 377–385.
[19] G.B. Schulz, et al., Therapeutic and prognostic implications of NOTCH and MAPK signaling in bladder cancer, Cancer Sci. 112 (5) (2021) 1987–1996.
[20] A.C. Hepburn, et al., Side population in human non-muscle invasive bladder cancer enriches for cancer stem cells that are maintained by MAPK signalling, PLoS One 7 (11) (2012) e50690.
[21] M. Yanchun, et al., Triptolide prevents proliferation and migration of Esophageal Squamous Cell Cancer via MAPK/ERK signaling pathway, Eur. J. Pharmacol. 851 (2019) 43–51.
[22] Y. Cakir, Human estrogen sulfotransferase (EST) enzyme modulates MAPK pathway in human BreastT cancer cell line MCF-7, Journal of Applied Bioloical Sciences 12 (1) (2021) 115–125.
[23] I.A. Mayer, et al., The p38 mapk pathway mediates the growth inhibitory effects of interferon- in bcr-abl-expressing cells, J. Biol. Chem. 2001 (30) (2001) 28570–28577.
[24] Y. Min Hee, et al., Brassinin induces apoptosis, autophagy, and paraptosis via MAPK signaling pathway activation in chronic myelogenous leukemia cells, Biology 12 (2023) 307–320.
[25] J.H. Yen, et al., Nobiletin promotes megakaryocytic differentiation through the MAPK/ERK-Dependent EGR1 expression and exerts anti-leukemic effects in human chronic myeloid leukemia (CML) K562 cells, Cells 9 (4) (2020) 877.
[26] C. Jinhao, et al., Gambogic acid induces death of K562 cells through autophagy and apoptosis mechanisms, Leuk. Lymphoma 56 (2015).
[27] S. Xianping, et al., Gambogic acid induces apoptosis in imatinib-resistant chronic myeloid leukemia cells via inducing proteasome inhibition and caspase-dependent Bcr-Abl downregulation, Clin. Cancer Res. : an official journal of the American Association for Cancer Research 20 (2013).
[28] H. Huey-Lan, et al., Induction of apoptosis and differentiation by atractylenolide-1 isolated from Atractylodes macrocephala in human leukemia cells, Bioorg. Med. Chem. Lett 26 (2016).
[29] A. Yehai, et al., Chemoproteomics reveals glaucocalyxin A induces mitochondria-dependent apoptosis of leukemia cells via covalently binding to VDAC1, Advanced biology 8 (2023).
[30] L. Jun, et al., Dihydroartemisinin inhibits the Bcr/Abl oncogene at the mRNA level in chronic myeloid leukemia sensitive or resistant to imatinib, Biomed. Pharmacother. 67 (2012).
[31] K. Banik, et al., Wogonin and its analogs for the prevention and treatment of cancer: a systematic review, Phytother Res. : PT 36 (5) (2022) 1854–1883.
[32] M. Mehdi, et al., Wogonin inducing apoptosis in breast cancer cell line, Immunoregulation 4 (3) (2021) 33–42.
[33] M.H. Nazmy, et al., Assessing the antiproliferative potential of a novel combretastatin A4 derivative via modulating apoptosis, MAPK/ERK and PI3K/AKT pathways in human breast cancer cells, FBL 28 (8) (2023) 185.
[34] H. Cao, et al., Wogonin reverses the drug resistance of chronic myelogenous leukemia cells to imatinib through CXCL12-CXCR4/7 axis in bone marrow microenvironment, Ann. Transl. Med. 8 (17) (2020) 1046.
[35] X. Liu, et al., LW-213, a newly synthesized flavonoid, induces G2/M phase arrest and apoptosis in chronic myeloid leukemia, Acta Pharmacol. Sin. 41 (2) (2019) 249–259.
[36] H. Xing, et al., Determination of GL-V9, a derivative of wogonin, in rat plasma by UPLC-MS/MS and its application to a pharmacokinetic study after oral and pulmonary administration, Biomed. Chromatogr. 33 (8) (2019) e4556.
[37] L. Li, et al., GL-V9, a newly synthetic flavonoid derivative, induces mitochondrial-mediated apoptosis and G2/M cell cycle arrest in human hepatocellular carcinoma HepG2 cells, Eur. J. Pharmacol. 670 (1) (2011) 13–21.
[38] W. Rui, et al., GL-V9 inhibits the activation of AR-AKT-HK2 signaling networks and induces prostate cancer cell apoptosis through mitochondria-mediated mechanism, iScience 27 (2024).
[39] G. Yabing, et al., GL-V9 ameliorates liver fibrosis by inhibiting TGF-β/smad pathway, Exp. Cell Res. (2023) 425.
[40] E. Lugli, et al., Characterization of cells with different mitochondrial membrane potential during apoptosis, Cytometry 68 (1) (2018) 28–35.
[41] Yu, Y.L.R.L.Z.B.L.Z, Pristimerin induces autophagy-mediated cell death in K562 cells through the ROS/JNK signaling pathway, Chem. Biodivers. 16 (8) (2019) e1900325.
[42] C. Hegedus, et al., Distinct interaction profiles of the second generation Bcr-Abl inhibitors nilotinib and bosutinib with the ABCG2 multidrug transporter, Cancer Res. 68 (2008).
[43] S. Aggarwal, et al., Voice of cancer patients: patient experience regarding use of tyrosine kinase inhibitors in chronic myeloid leukemia, Blood 134 (Supplement_1) (2019), 5843-5843.
[44] Rui . Wang, et al., GL-V9 inhibits the activation of AR-AKT-HK2 signaling networks and induces prostate cancer cell apoptosis through mitochondria-mediated mechanism, Science 27 (3) (2024).
[45] J. Liu, et al., Inhibition of TRPV4 remodels single cell polarity and suppresses the metastasis of hepatocellular carcinoma, Cell Death Dis. 14 (6) (2023) 379.
[46] A.D. Cristofano, et al., P62dok, a negative regulator of ras and mitogen-activated protein kinase (Mapk) activity, opposes leukemogenesis by P210bcr-abl, J. Exp. Med. 194 (3) (2001) 275–284.
[47] Y. Lee, J. Chiou, L. Chang, AMPK inhibition induces MCL1 mRNA destabilization via the p38 MAPK/miR-22/HuR axis in chronic myeloid leukemia cells, Biochem. Pharmacol. 209 (2023) 115442.